IIETA International Information and Engineering Technology Association
Advancing the World of Information and Engineering

Annales de Chimie - Science des Matériaux
Vol. 50, No. 1, February, 2026, pp. 43-56
Journal homepage: http://iieta.org/journals/acsm

Mechanical Properties of Sand Concrete Containing Recycled Marble Powder and Steel Fibres at Ambient and Elevated Temperatures

Yasser Mohamed Aimen Zeltni[1], Nadia Otmani-Benmehidi[1*], Abdessalam Otmani[2], Ali Ourdjini[3]

[1] Materials, Geomaterials and Environment Laboratory, Faculty of Technology, Badji Mokhtar-Annaba University, Annaba 23000, Algeria
[2] Department of Process Engineering and Energetics, National Higher School of Technology and Engineering, Annaba 23005, Algeria
[3] Faculty of Engineering, University of Ottawa, Ottawa K1N 1A2, Canada

Corresponding Author Email: nadia.otmani@univ-annaba.dz

https://doi.org/10.18280/acsm.500105

Received: 30 November 2025
Revised: 6 February 2026
Accepted: 14 February 2026
Available online: 28 February 2026

Keywords:
ecological concrete, materials recycled, mechanical properties, sand concrete, waste recovery

ABSTRACT

The intensive extraction of natural sand to meet the demands of urbanization has led to significant environmental damage and resource depletion. Consequently, increasing attention has been directed toward the use of industrial waste materials as partial replacement for natural aggregates in concrete, driven by both ecological and economic benefits. In Algeria, the marble industry generates substantial quantities of waste during the manufacturing process, creating an opportunity for sustainable reuse. This study investigates the mechanical performance of sand concrete incorporating marble waste sand as a partial substitute for quarry sand and steel fibres as reinforcement, evaluated at ambient temperature and after exposure to 600 °C. Quarry sand was replaced by marble waste sand at a fixed rate of 40%, while steel fibres were added at volume fractions of 0%, 0.25%, 0.50%, and 0.75%. The results demonstrate that the combined use of marble waste sand and steel fibres significantly improves the properties of sand concrete under both ambient and elevated high temperature conditions. These findings highlight the potential of this composite as a sustainable and high-performance alternative for the construction industry.

1. INTRODUCTION

Rapid urbanization has led to an unprecedented demand for sand, which is extensively extracted from rivers and mountainous regions. This excessive exploitation has caused significant resource depletion and severe environmental degradation [1], adversely impacting ecosystems and prompting global research efforts to explore sustainable alternatives to natural sand in concrete, particularly using waste materials [2-4]. Among these alternatives, glass has been identified as a high-quality and sustainable substitute for natural sand in concrete production, as demonstrated by the findings of Dadouch et al. [5]. Previous studies have examined various aspects of concrete modifications. Ravina and Mehta [6] investigated the impact of fly ash on compressive strength and reported substantial improvements in concrete performance, particularly in lean mixtures. Furthermore, according to Wang et al. [7], the incorporation of biochar as a 100 vol% replacement for sand reduced concrete shrinkage by 65% at 28 days while ensuring improved long-time strength development. Marble powder has also been extensively studied as a potential replacement for natural sand in concrete, with numerous investigations reporting its effectiveness [8-14].

Although the effects of cement substitution and steel fibre addition have been studied independently, limited research has addressed their combined impact on the performance of sand concrete. In accordance with the relevant standard [15], sand concrete is a cement-based material composed exclusively of fine aggregates (≤ 5 mm), without coarse aggregates. Owing to this composition, it exhibits a denser and more homogeneous structure than conventional concrete and demonstrates superior mechanical properties compared to mortar [16]. These characteristics make sand concrete an effective material for structural applications requiring high compactness, good workability, and reliable mechanical performance. When reinforced with fibres, sand concrete becomes a high-performance composite material in which the fibres play a crucial role in enhancing mechanical properties [17]. Fibre reinforcement improves tensile/flexural strength, ductility, and toughness through crack-bridging mechanisms, while also reducing shrinkage cracking and enhancing durability. The homogeneous, aggregate-free microstructure ensures uniform fibre dispersion [18]. In addition, fibres contribute to improved thermal resistance at high temperatures by mitigating spalling and helping to preserve structural integrity, making fibre-reinforced sand concrete particularly suitable for demanding applications, including structures exposed to fire.

Regarding the effect of marble waste, Bayraktar et al. [19]

reported that substituting silica sand with waste marble powder (WMP) in foamed concrete significantly enhances mechanical properties, including compressive, tensile, and flexural strengths, while reducing drying shrinkage by up to 25.55%. Similarly, Shukla et al. [20] found that replacing cement with marble dust yields optimal strength at approximately 15%; however, beyond this level, strength decreases and brittleness increases. In a related study, Venkataramana and Babu [21] investigated marble waste as a coarse aggregate replacement and observed a gradual decline in strength with increasing substitution levels up to 50%. To address these limitations, several studies have highlighted the effectiveness of fibre reinforcement. Bayraktar et al. [19] demonstrated that incorporating basalt fibres improves mechanical performance and crack control, with an optimal fibre content of around 1%. Likewise, Venkataramana and Babu [21] showed that adding 1-2% steel fibres effectively compensates for strength loss caused by high marble waste content while enhancing ductility. Karimipour et al. [22] further showed that marble slurry powder (MSP), due to its high fineness and filler effect, contributes more significantly to compressive strength than other fillers. However, its effect on tensile strength is limited unless combined with fibres. The incorporation of steel fibres (0.1–0.2%) significantly improves both compressive and especially splitting tensile strength through crack-bridging mechanisms and enhanced ductility. Overall, the combined use of MSP and steel fibres results in a denser microstructure and superior mechanical performance.

The present work investigates a novel sand concrete composite incorporating recycled marble powder as filler and steel fibres as reinforcement, evaluated under both ambient conditions and elevated temperature exposure up to 600 °C. A temperature of 600 °C was selected as a representative high temperature exposure because it lies just above the critical threshold at which concrete typically experiences a 50–60% reduction in strength and the onset of pronounced visible cracking. In a previous study by the authors (currently under publication), sand-based concrete without steel fibres was exposed to 20 °C, 150 °C, 300 °C, 450 °C, 600 °C, and 800 °C. The results showed that at 600 °C, the concrete retained only minimal residual strength, while at 800 °C it had deteriorated to a condition unsuitable for mechanical testing. These observations are consistent with the findings of Phan and Carino [23], who reported that both compressive strength and tensile strength decrease markedly beyond 400–600 °C, with damage particularly severe above 600 °C. The use of waste marble, either as an aggregate or as an admixture, has been shown to enhance concrete durability, confirming its suitability for both conventional and self-compacting concrete (SCC) mixes [23, 24]. Vardhan et al. [25] further demonstrated that waste marble improves mechanical strength, permeability resistance, and microstructural characteristics of concrete, with optimal performance achieved at a 40% replacement. The addition of steel fibres into manufactured sand concrete (MSC) has attracted significant research interest. Sand concrete, as a quasi-brittle material, inherently exhibits low tensile strength and poor crack resistance, which limit its structural applications.

The inclusion of steel fibres effectively inhibits and reduces the propagation of macroscopic cracks [26], thereby improving the material's overall performance and durability. Cai et al. [27] investigated the fracture behaviour of steel fibre-reinforced manufactured sand concrete (SFRMSC) and demonstrated improvements in residual strength, fracture toughness, and fracture energy with increasing fibre volume fraction. Murali and Vinodha [28] assessed the impact of the failure strength of steel hybrid fibre reinforced concrete (SHFRC) under freeze-thaw cycles, highlighting the critical role of long fibres in enhancing strength. Ammari et al. [29] examined the durability of sand concrete with lignocellulosic and steel hybrid fibres, showing enhanced performance under severe conditions with increasing steel fibre content. Jiao et al. [30] also reported superior mechanical and fracture properties in SFRMSC compared to conventional mixes. The addition of fibres was found to reduce fluctuations in the acoustic parameter, with a steel fibre content of 1% yielding the highest flexural strength. Durgun and Sevinc [31] investigated the effects of replacing conventional limestone aggregate with basalt, barite, marble, and pumice on the engineering properties and durability of concrete. The produced specimens were subjected to comprehensive testing, including unit weight, compressive strength, splitting tensile strength, ultrasonic pulse velocity (UPV), water absorption, and apparent porosity. Furthermore, high-temperature performance was assessed by exposing the specimens to temperatures of 600 °C and 800 °C. SCC is increasingly used in high-rise and industrial buildings, which are particularly vulnerable to fire hazards due to dense electrical and gas systems. Ahmad et al. [32] evaluated the performance of SCC after exposure to 500 °C.

Post-exposure evaluation included visual inspection for cracking and spalling, along with measurements of mass loss, compressive strength, and tensile strength. Their results indicated that the addition of steel fibres improved the performance of SCC at elevated temperatures. In contrast, the control mix without steel fibres exhibited considerable degradation when exposed to 500 °C. Although the effect of high temperatures on concrete has been extensively studied, sand concrete containing marble powder and steel fibres remains largely unexplored. In Algeria, the marble manufacturing industry generates substantial quantities of waste, yet recycling rates remain very low. From environmental, economic and safety perspectives, this study aims to evaluate sand concrete formulated by replacing 40% of cement with WMP as filler and incorporating steel fibres at different volume fractions (0%, 0.25%, 0.50%, 0.75%). Accordingly, the key and novel objective of the present work is to investigate the behaviour of a new sand concrete composite incorporating recycled marble powder filler and steel fibre reinforcement, under two conditions: ambient temperature and exposure to 600 °C.

2. EXPERIMENTAL PROCEDURES

2.1 Materials used

The cement used in this study was Portland CEM I/42.5 cement, of Algerian origin, supplied by SPA BISKRIA cement, whose main chemical and physical properties of cement are summarised in Tables 1 and 2, respectively. Marble fines used as filler were sourced from the Filfila quarry, located east of Skikda, in northeastern Algeria. The marble powder is a by-product of the marble extraction and processing operations, generated from residues and waste produced during marble manufacturing.

Table 1. Physical characteristics of cement CPA-CEM I/42.5

Physical Characteristics		Cement CPA
Absolute density	3.10 g/m^3	
Apparent density	0.9 g/m^3	
Blaine surface	3000	cm^2/g
Start of taking	150–190	min
End of take	220–250	min
Normal consistency	25.8–26.4	%
Lime expansion	0.25–1.0 mm	

Table 2. Chemical composition of cement CPA-CEM I/42.5

Element	Percentage (%)
SiO_2	21
Al_2O_3	4.41
Fe_2O_3	3.62
CaO	63.76
MgO	1.7–2.8
SO_3	2.2–2.8
Na_2O	0.16
K_2O	0.47
Cl	0.03–0.07

Its physical characteristics and chemical composition are illustrated in Tables 3 and 4, respectively. The sand used in this study was a blend of quarry sand (0/5) and siliceous sand to achieve a particle size distribution conforming to standard specifications. The sand mixture consisted of 75% quarry sand and 25% siliceous sand. The siliceous sand was classified as 0/2 and sourced from Tebessa, in northeastern Algeria, while the limestone quarry sand of class 0/5 was extracted from the Guelma quarry, also located in northeastern Algeria. The physical and chemical properties of both aggregates are presented in Table 5. The particle size distributions of the two sand types are shown in Figure 1.

Table 3. Physical characteristics of marble powder

Physical Properties	Marble Powder
Absolute density (g/m^3)	2.72
Apparent density (g/m^3)	1.02
Blaine surface (cm^2/g)	3800

Table 4. Chemical composition of marble powder

Element	SiO_2	Al_2O_3	Fe_2O_3	CaO	MgO	P.C
Percentage (%)	0.15	0.08	0.04	54.86	1.03	44.26

Table 5. Physical properties of sand

Physical Properties		Siliceous Sand	Quarry Sand
Dimensions d/D	mm/mm	0/2	0/5
Absolute density	g/m^3	2.65	2.59
Apparent density	g/m^3	1.457	1.403
Inter granular porosity	%	45.02	45.83
Fineness module	-	1.66	3.07
Sand equivalent	%	73.77	79.20

The steel fibres used were DRAMIX 3D RC-65/50-BL, conforming to the EN 14889-1 standard. Their physical and mechanical properties, as provided by the manufacturer, are summarised in Table 6. A water-reducing superplasticizer, 'Visco Crete®-522 RMX' [Société SIKA Algérie], was used as an adjuvant and is supplied as a dark brown liquid with a pH of approximately 5 and a density of 1.085. The dosage was varied between 0.4% and 2.5% by weight of the binder.

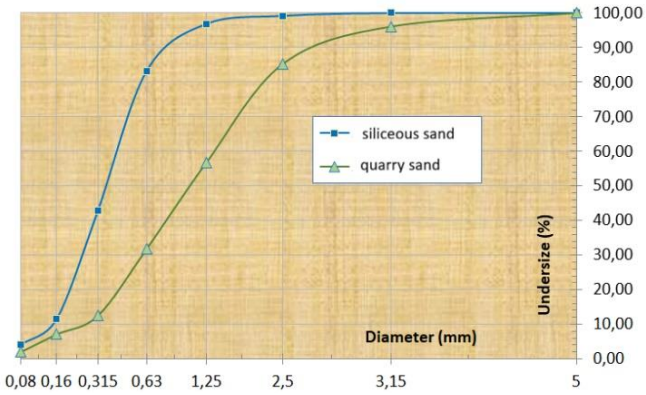

Figure 1. Particle size distribution curves

Table 6. Physical and mechanical properties of metal fibres

Physical Characteristics		Metal Fibres
Length	mm	50
Diameter	mm	0.75
Fiber elongation	-	65
Modulus of elasticity	N/mm²	1.225
Tensile strength	N/mm²	210000
Density	Kg/m^3	7850
Ductility of the wire	%	0.8

2.2 Sand concrete formulation

Sand concrete, free of gravel in accordance with NF P 18-500, differs from mortar by its lower cement content, the presence of fine particles, and the use of a water-reducing plasticizer. As a structural material, it exhibits performance levels comparable to those of traditional concretes. The concrete used in this experimental phase is a sand concrete. Its formulation follows the sandblasting method [33], which determines the proportions of the various constituents for a fixed cement content of 355 kg/m^3 and a water-to-cement ratio (w/C) of 0.60. The concrete achieved a consistency class of S2, characterized by a slump of 5-9 cm measured using the Abrams cone test, in accordance with standard NF P 18-451. Table 7 presents the composition per cubic meter of concrete:

Table 7. Composition of sand concretes studied [kg/m^3]

	Sand Concrete	Fibre Sand Concrete 0.25%	Fibre Sand Concrete 0.50%	Fibre Sand Concrete 0.75%
Dune sand	309.65	308.88	308.10	307.33
Quarry sand	1210.57	1207.54	1204.51	1201.49
Water	212.95	212.95	212.93	212.93
Cement	354.85	354.85	354.85	354.85
Filler	144.65	144.65	144.65	144.65
Super plasticizer	3.52	3.52	3.52	3.55
Metal fibre	0.00	11.47	22.93	34.40
W/C	0.60	0.60	0.60	0.60

2.3 Preparation and storage of test samples

The test specimens were prepared in accordance with the standard [34]. The concrete was mixed in a mechanical mixer for 5 minutes in Figures 2(a) and (b). Workability was evaluated using the widely adopted Concrete Slump Test in Figure 2(c).

In this test, the slump cone is filled in three layers with fresh concrete in three equal layers, each compacted with 25 strokes of a standard tamping rod. After carefully lifting the cone vertically, the resulting decrease in height of the concrete is measured. This value, known as the slump, indicates the fluidity of the mix. To ensure proper compaction and minimise air voids, the mixture was vibrated on a vibrating table for 1 minute (Figure 2(d)). It was then cast into metal moulds to produce cubic specimens with the dimensions 10 × 10 × 10 cm for compression strength tests and prismatic specimens (4 × 4 × 16 cm and 7 × 7 × 28 cm) for flexural tensile tests (Figure 2(e) and (f)). The specimens were kept in their moulds for 24 hours under laboratory conditions at a temperature of approximately 20 °C ± 2 °C. After the initial curing period, the specimens were demoulded and immersed in water at 20 °C (Figure 2(f)) until the testing date, in accordance with NF P 18-404 standard. This curing procedure promotes cement hydration and ensures the integrity of the samples for subsequent testing. Figure 3 shows the test specimens investigated in the present work.

Figure 2. Test specimen preparation (a) mechanical mixing, (b) mixing of the concrete in the mechanical mixer, (c) slump test for workability of fresh concrete, (d) preparation of concrete specimens in moulds on a vibrating table, (e) concrete specimens in moulds, (f) the specimens in the water

Figure 3. Test specimens

Figure 4. Heating of test specimens inside the furnace

2.4 Fire tests

2.4.1 Thermal cycling

The initial ambient temperature was set to 20 °C. The specimens were heated at a controlled rate of 2 °C/min until reaching the target temperature of 600 °C. This temperature was maintained for 1 hour to ensure uniform thermal distribution throughout the specimens. After the heating phase, controlled cooling was carried out inside the furnace until the specimens returned to ambient temperature. All heat treatments were performed using an instrumented electric furnace, as shown in Figure 4. The selected maximum temperature of 600 °C was chosen to evaluate critical thresholds associated with structural degradation and phase transformations within the cement matrix under high temperature exposure [35, 36].

2.4.2 Mechanical testing

Specimens were classified into two groups: unheated and heat-treated (exposed to 600 °C for 1 hour). Mechanical testing was conducted on the unheated specimens after 7, 14, and 28 days of curing, whereas the heat-treated specimens were tested only after 28 days. In addition, ultrasonic velocity measurements were taken on all specimens in accordance with the procedure outlined in this study [37] (Figure 5). Mechanical properties were assessed by conducting compressive strength tests (Figure 6(a)) and three-point bending tests (Figure 6(b)) on the prepared specimens. The compressive strength tests were conducted in accordance with the standard [38] using 10 × 10 × 10 cm cubic specimens. All tests were carried out with a digital 'Digitec' testing machine. The three-point bending tensile test was conducted as defined in the relevant standard [39], using the prismatic specimens measuring 4 × 4 × 16 cm and the 7 × 7 × 28 cm.

Figure 5. Ultrasonic testing of concrete specimens

Figure 6. Mechanical properties testing (a) compression test specimens, (b) three-point bending test specimen

The tests are performed on digital 'Digitec' testing machine located in the laboratories of the Institute of Civil Engineering at Badji Mokhtar University (Annaba, Algeria). During testing, each specimen was carefully positioned on the lateral supports, with particular attention given to longitudinal alignment. The load was applied precisely at the mid-point to ensure uniform stress distribution. Proper seating of the specimen was verified prior to loading to prevent instability, misalignment, or tipping.

3. RESULTS AND DISCUSSION

3.1 Slump test and density of sand concrete

Figure 7 illustrates the variation in slump values for the reference sand concrete and fibre-reinforced sand concrete containing 0.25%, 0.50%, and 0.75% fibres. The reference sand concrete exhibits the highest slump value at 8.5 cm, indicating good workability. Incorporating 0.25% fibres slightly reduces the slump to 8 cm, reflecting a minor decrease in workability while remaining within acceptable handling limits. As the fibre content increases to 0.50%, the slump further decreases to 7.3 cm, indicating a more noticeable reduction in workability. At 0.75% fibre content, the slump reaches 7 cm, representing the lowest workability among all mixtures tested. These results show a clear inverse relationship between fibre content and workability. The progressive reduction in slump with increasing fibre content can be attributed to increased friction and entanglement of the fibres within the matrix. Adequate fibre dispersion was ensured despite the limitations of the slump test, which reflects yield stress but not viscosity, the latter being critical for fibre dispersion. Accordingly, for the sand-based concrete containing 0.75% steel fibres, the amount of superplasticizer was increased to achieve an acceptable slump of approximately 7 cm.

Figure 8 shows the variation in the 28-day density of fresh cured concrete for the reference sand concrete and the fibre-reinforced mixtures samples containing 0.25%, 0.50%, and

0.75% fibres. The reference sand concrete exhibits the lowest density, measured at 2.235 g/m³. Addition of 0.25% fibres leads to a notable increase in density to 2.319 g/m³, indicating improved compactness. This upward trend continues at 0.50% fibre content, where the density reaches 2.329 g/m³, though the rate of increase becomes less pronounced. At 0.75% fibre content, the density further rises slightly to 2.337 g/m³, suggesting diminishing gains with higher fibre content. Overall, the results demonstrate that fibre addition contributes to an increase in the density of sand concrete as previously confirmed by Wang and Niu [40].

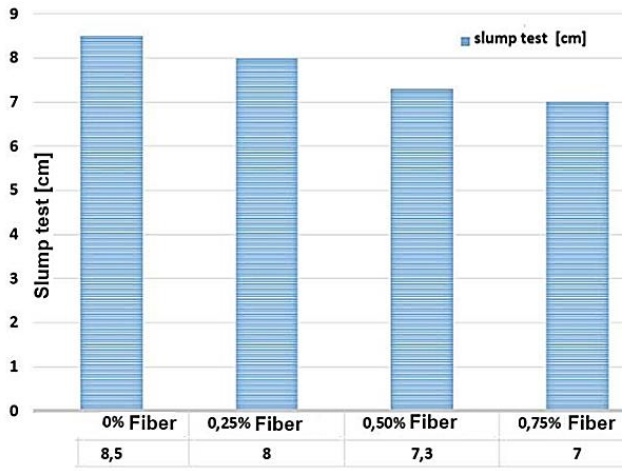

Figure 7. Variation of slump sand concrete

However, the effects become less pronounced as fibre content increases, indicating a potential saturation threshold beyond which further fibre addition yields limited benefits in terms of density enhancement.

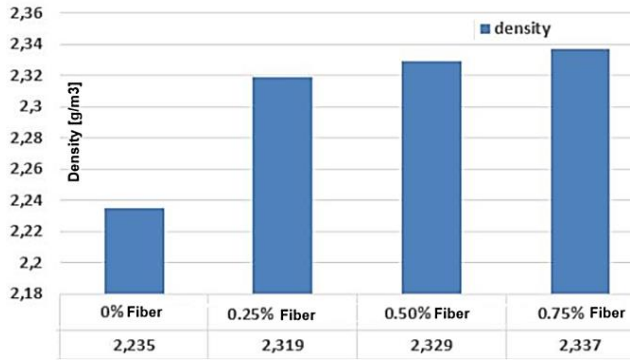

Figure 8. Density variation of fresh cured concrete at 28 days

3.2 Mechanical characterization of unheated specimens

Table 8 shows the mechanical properties of the developed sand concrete composite incorporating recycled marble powder as filler and steel fibre reinforcement at ambient temperature. The statistical analysis of the compressive strength at 20 ℃ as function of fibre content for the various curing ages are tabulated in Tables A1-A4. The results clearly demonstrate the effectiveness of this incorporation strategy in enhancing the overall performance of sand concrete. Previous studies support these findings. For instance, Kabbo et al. [41] reported that implementing different proportions of marble powder with a fixed amount of steel fibres significantly enhanced the mix's flowability, passing ability, and viscosity. Furthermore, the same study indicated that a combination of 10% WMP and 5% silica fume (SF) produced a linear increase in both compressive strength and splitting tensile strength. In addition, Ahmad and Zhou [42] demonstrated that the incorporation of steel fibres and marble waste considerably enhanced the performance of SCC under aggressive environmental conditions.

Table 8. Mechanical properties of unheated specimens

Fibre Content, %	Age, Day	Temperature, ℃	Compressive Strength, N/mm²	Flexural Strength N/mm²	Ultrasonic Velocity, m/s
0	28	20	42.24	8.42	4494
0.25	28	20	39.18	9.36	4535
0.5	28	20	44.84	8.51	4505
0.75	28	20	45.06	8.58	4230

3.2.1 Compression strength

Figure 9 presents steel fibre-reinforced concrete samples containing different fibre contents (0.25%, 0.5% and 0.75%) following compression testing at 7 aging days. Figure 10 shows the development of compressive strength in sand concrete samples incorporating different steel fibre contents (0%, 0.25%, 0.50% and 0.75%), measured at curing ages of 7, 14 and 28 days. For all mixtures, compressive strength increases with curing time, reflecting the hardening process of concrete. The incorporation of steel fibres enhances compressive strength compared with the reference mix, with the most pronounced improvement observed at a fibre content of 0.50%.

Beyond 0.50% fibre content, strength gains tend to plateau, indicating that higher fibre contents do not lead to further significant improvements in compressive strength. This trend is consistent with findings reported in the literature [43], where an optimal combination of 1% steel fibres and 15% marble dust as a cement replacement produced the highest mechanical strength, while higher contents resulted in significant strength reduction.

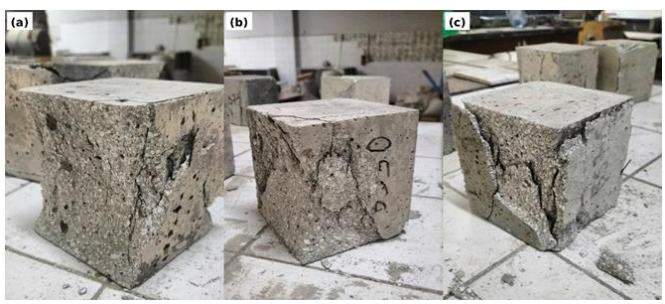

Figure 9. Test specimen after compression test, (a) BS25, (b) BS50, (c) BS75

In the present study, sand concrete incorporating marble waste as partial aggregate replacement and 0.50% steel fibres

provides favourable balance between mechanical performance and material efficiency. The results indicate that a moderate steel fibre content of approximately 0.50% is optimal for maximising compression strength.

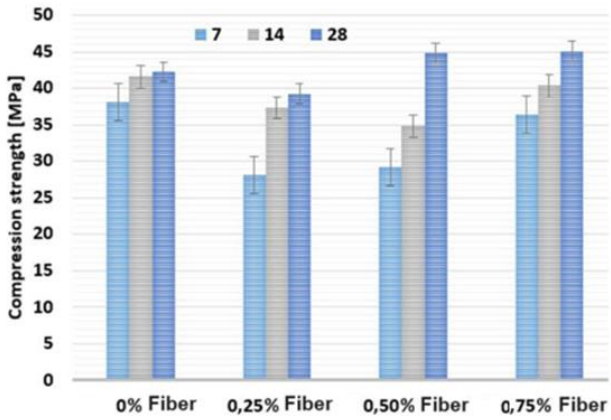

Figure 10. Compressive strength of sand concrete incorporating marble filler, with and without steel fibre reinforcement

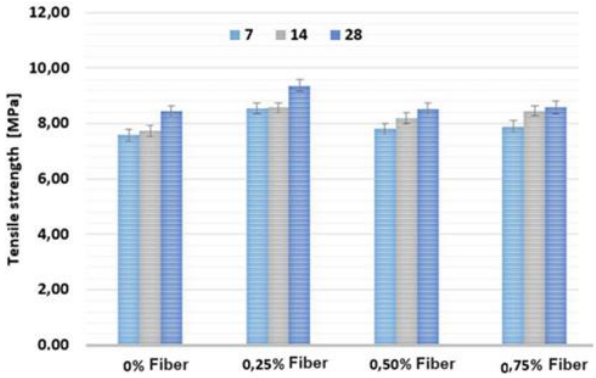

Figure 11. Tensile strength of sand concrete incorporated with marble filler, with and without steel fibre reinforcement

3.2.2 Tensile strength

Figure 11 illustrates the evolution of tensile strength for sand concrete mixes with and without steel fibres, measured at curing ages of 7, 14 and 28 days. The fibre-free sand concrete exhibits a gradual increase in bending strength increases with time, reaching about 8.5 MPa at 28 days, which confirms continued strength development after the initial hardening period, albeit at a lower level than fibre-reinforced mixtures. The incorporation of 0.25% steel fibres always leads to a slight but consistent improvement in bending strength, achieving about 9 MPa at 28 days. Increasing the fibre content to 0.50% does not result in a proportional gain, as the flexural strength at 28 days remains comparable to, or slightly lower than, that of the 0.25% fibre mixture, although a steady improvement is observed during early hardening. A further increase to 0.75% fibre content yields similar results with a strength around 9 MPa at 28 days, indicating that beyond a certain threshold the contribution of additional fibres becomes marginal and may even stagnate. This behaviour is in line with findings reported in the literature [27], which suggests that higher fibre contents enhance aggregate-matrix but can also promote the formation of microcracks, limiting further strength gains. Overall, while steel fibre addition improves the mechanical properties of sand concrete, these results highlight the importance of optimising fibre dosage to maximize performance while controlling material costs. The statistical analysis of the tensile strength at 20 ℃ as function of fibre content for the various curing ages are shown in Tables A5-A8.

3.3 Residual characteristics of heated specimens

Table 9 summarises the results of the residual properties of steel fibre-reinforced sand concrete with fibre contents of 0%, 0.25%, 0.50%, and 0.75%. According to the findings reported in this study [27], although the incorporation of steel fibres enhances the post-peak behaviour of sand concrete, it may also increase the presence of initial defects such as pores and bond interfaces. The statistical analyses of compressive strength and mass loss as functions of fibre content at 600 °C are reported in Tables A9 and A10, respectively, whereas Tables A11 and A12 report the corresponding analyses for tensile strength and ultrasonic velocity at 600 °C.

Table 9. Residual mechanical characteristics of specimens heated at 600 ℃

Fibre Content, %	Compressive Strength, N/mm²	Flexural Strength, N/mm²	Mass Loss, %	Ultrasonic Velocity, m/s
0	26.96	1.95	8.88	2177
0.25	24.66	3.5	8.48	1923
0.5	26.57	2.62	7.91	2092
0.75	22.01	2.77	6.84	2017

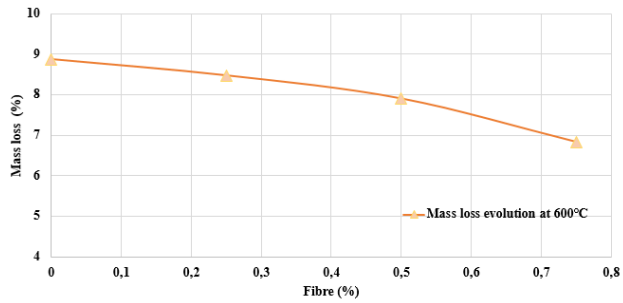

Figure 12. Mass loss of fibre-reinforced sand concrete after exposure to 600 ℃

3.3.1 Mass loss of fibred sand concrete

As shown in Figure 12, a significant mass loss is observed at 600 ℃, primarily attributed to the evaporation of free and bound water as well as the progressive decomposition of cement hydration products. In fibre-free sand concrete, uncontrolled thermal cracking promotes rapid vapor migration, resulting in severe matrix damage that is often accompanied by localized spalling and marked surface degradation. The addition of fibres contributes to controlling the initiation and propagation of thermal microcracks, promoting a more gradual release of water vapor and reducing the buildup of internal pressure. This mechanism decreases the effective permeability of the material during heating and mitigates spalling, resulting in a systematic reduction in mass loss with increasing fibre content. Visual observations of the specimens after fire exposure support this trend: fibre-free sand concrete displays extensive surface damage with open cracks and spalled zones, whereas fibre-reinforced sand concrete exhibits finer, more uniformly distributed microcracks and a comparatively stable surface. These macroscopic observations are consistent with the measured

mass loss results and confirm the beneficial role of fibres in improving the overall thermal stability of sand concrete, in agreement with findings reported in this study [43], which demonstrated that polypropylene and/or steel fibres reduce spalling and physical degradation in high-performance concrete exposed to elevated temperatures.

3.3.2 Flexural strength

In contrast to the behaviour observed in compression, the flexural strength (Figure 13) of sand concrete is significantly enhanced by the addition of fibres, even after exposure to 600 °C. Fibre-free sand concrete exhibits very low flexural strength (1.95 N/mm²), reflecting a brittle behaviour governed by rapid and uncontrolled crack propagation. At a low fibre content of 0.25%, the flexural strength increases markedly to 3.50 N/mm², corresponding to an improvement of approximately 80% compared with the reference sand concrete. This pronounced gain highlights the effectiveness of the crack-bridging mechanism widely reported in the literature, whereby fibres carry tensile stresses after matrix cracking, delay the initiation and propagation of thermally induced cracks, and enhance the residual ductility of the material.

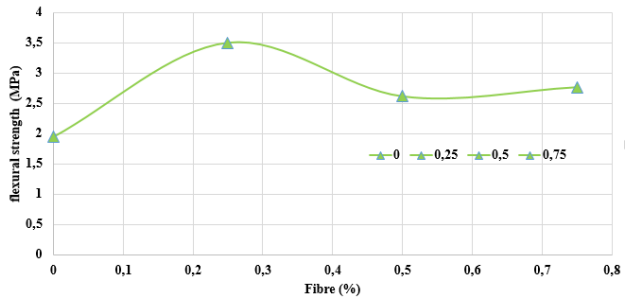

Figure 13. Effect of fibre content on flexural strength after exposure to 600 °C

For higher fibre contents (0.50% and 0.75%), the flexural strength remains higher than that of the fibre-free concrete, although the measured values are lower than the peak observed at 0.25%. This non-monotonic evolution reflects a balance between the beneficial effects of crack bridging and the adverse consequences associated with higher fibre content, such as partial thermal degradation of fibres, degradation of the fibre–matrix bond, and less homogeneous fibre dispersion or local fibre agglomeration. The slight recovery observed at 0.75% (2.77 N/mm²) further suggests the influence of random fibre dispersion, a phenomenon frequently reported in experimental studies on fibre-reinforced concrete and known to cause fluctuations in residual flexural strength.

Overall, these results confirm that fibres retain a significant residual effectiveness in flexure at elevated temperatures, with improved post-cracking behaviour and toughness remaining the dominant contribution. These findings are consistent with those reported in this study [44], who showed that even after exposure to temperatures as high as 600–800 °C, fibres significantly enhance post-cracking behaviour by limiting crack opening and propagation and maintaining higher residual flexural strength than fibre-free sand concrete. The observed reduction in residual flexural strength at higher fibre content is also in agreement with previous studies [31], which attribute the non-monotonic evolution of residual flexural strength to fibre clumping, random dispersion, and partial thermal degradation.

3.3.3 Compressive strength

At an exposure temperature of 600 °C, the residual compressive strength (Figure 14) of sand concrete shows an overall decreasing trend with increasing fibre content, although this evolution is not strictly monotonic. The fibre-free sand concrete exhibits the highest residual compressive strength (25.20 N/mm²), which can be attributed to an initially more compact and homogeneous cementitious matrix, free from additional discontinuities related to fibre–matrix interfaces. The incorporation of 0.25% fibres results in a significant decrease in compressive strength, primarily due to thermal degradation of the cement matrix in the 400–600 °C range, including the dehydroxylation of portlandite ($Ca(OH)_2$), partial decomposition of cement hydrates, and increased porosity. Under these conditions, the fibre-matrix interfaces act as preferential zones for crack initiation and propagation, thereby limiting the effectiveness of fibres under compressive loading despite their beneficial role in tension. At a fibre content of 0.50%, a slight recovery in compressive strength is observed (26.57 N/mm²), suggesting the presence of an optimal intermediate content at which fibres contribute to partial microcrack bridging and improved local stress redistribution without inducing excessive porosity. Similar observations have been reported in the literature for fibre-reinforced concretes exposed to 600 °C, where moderate fibre contents help restrain the coalescence of thermally induced microcracks.

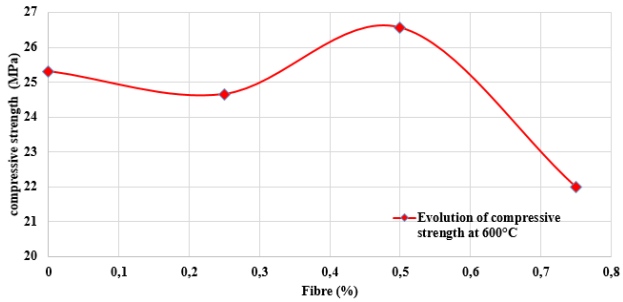

Figure 14. Effect of fibre content on compressive strength after exposure to 600 °C

In contrast, increasing the fibre content to 0.75% results in a more pronounced decrease in compressive strength (22.00 N/mm²), which is generally associated with aggravated thermal damage, arising from the accumulation of voids left by fibre degradation, non-uniform fibre distribution, and an overall weakening of the load-bearing matrix.

Thus, despite the localized crack-bridging effects at intermediate fibre contents observed at 0.50%, the overall influence of fibres on residual compressive strength at elevated temperatures remain unfavourable. These findings are consistent with the conclusions reported in this study [45], which showed that fibre addition, particularly polypropylene fibres, reduces residual compressive strength after exposure to 600 °C due to thermal degradation of the fibres and deterioration of the fibre–matrix interfaces.

3.3.4 Ultrasonic velocity

The UPV measured after exposure to 600 °C in Figure 15 shows a reduction compared with values typically recorded at ambient temperature, indicating significant internal

microstructural damage. All measured velocities fall within the range of 1923 to 2177 m/s, confirming that the concrete has been severely affected by high temperature exposure, since sound, undamaged concrete generally exhibits ultrasonic velocities exceeding 3500 m/s) [37]. The control sand concrete displays the highest pulse velocity of 2177 m/s, whereas fibre-reinforced concretes show slightly lower values, though without evidence of abrupt degradation despite the high-temperature exposure. This overall reduction in pulse velocity is mainly attributed to the formation of thermal microcracks and increased porosity. The drop observed at a fibre content of 0.25% fibre content (1923 m/s) correlates well with the corresponding decrease in compressive strength, suggesting an increase in porosity or internal microcracking, likely caused by fibre degradation at elevated temperatures.

The variations observed with different fibre contents suggest a dual role of fibres: while they introduce local discontinuities that tend to slow the propagation of ultrasonic waves, they also contribute to controlling the formation of major cracks. As a result, pulse velocity values for fibre-reinforced concrete remain within a relatively narrow range, indicating that, despite thermal exposure, the fibres provide a degree of microstructural stabilization by limiting the development of severe cracking.

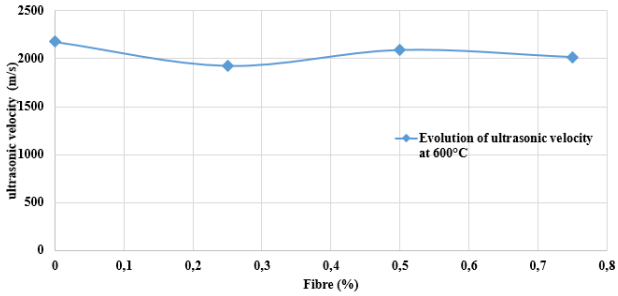

Figure 15. Effect of fibre content on ultrasonic velocity

4. CONCLUSIONS

- The incorporation of steel fibres systematically reduces mass loss by limiting the initiation and propagation of thermal microcracks. This promotes gradual vapor release, reduces internal pressure, mitigates spalling, and results in improved thermal stability and reduced surface degradation compared to reference concrete.
- Steel fibres significantly enhance flexural strength after high-temperature exposure. The optimum performance is achieved at a low fibre content (0.25%), with an increase of approximately 80%, due to effective crack-bridging. Higher fibre contents (0.50% and 0.75%) still outperform the reference concrete but exhibit a non-monotonic relationship, likely due to fibre degradation, bond deterioration, and dispersion issues at higher dosages.
- Under the investigated conditions, the residual compressive strength appears to be controlled primarily by thermal degradation of the matrix, while fibre addition plays a secondary role, mainly through its influence on porosity. As no quantitative porosity measurements were conducted in the present study, this interpretation is based on qualitative observations and is supported by trends in previous research, where similar porosity levels are associated with only minor variations in compressive strength. Fibre addition does not appear to cause significant degradation; however, a moderate fibre content (0.50%) provides a slight improvement, likely due to limited microcrack-bridging effects.
- All tested samples show a significant reduction in UPV, indicating severe internal microstructural damage induced by heating. Fiber-reinforced concretes show slightly lower velocities than the reference concrete, consistent with increased porosity from fibre degradation. Nevertheless, fibres restrict the development of macrocracks, resulting in relatively stable velocity values across different fibre contents.

Future research will focus on investigating the evolution of porosity in fibre-reinforced concrete after fire exposure and characterising thermally induced microcracking within the material. Attention will be given to correlating these microstructural changes with residual mechanical properties. This approach will provide deeper insight into the post-fire behaviour of fibre-reinforced concrete and support the optimization of its performance under elevated-temperature conditions.

ACKNOWLEDGEMENTS

The authors sincerely thank the Materials Geomaterials and Environment Laboratory (LMGE) of Badji Mokhtar University – Annaba and the Laboratory of Metallurgy at the National Higher School of Technology and Engineering (ENSTI-Annaba) for their valuable support and collaboration.

REFERENCES

[1] Gavriletea, M.D. (2017). Environmental impacts of sand exploitation. Analysis of sand market. Sustainability, 9(7): 1118. https://doi.org/10.3390/su9071118

[2] Tran, D.D., Thien, N.D., Yuen, K.W., Lau, R.Y.S., Wang, J., Park, E. (2023). Uncovering the lack of awareness of sand mining impacts on riverbank erosion among Mekong Delta residents: Insights from a comprehensive survey. Scientific Reports, 13(1): 15937. https://doi.org/10.1038/s41598-023-43114-w

[3] Bendixen, M., Best, J., Hackney, C., Iversen, L.L. (2019). Time is running out for sand. Nature, 571(7763): 29-31. https://doi.org/10.1038/d41586-019-02042-4

[4] Faried, A.S., Mostafa, S.A., Tayeh, B.A., Tawfik, T.A. (2021). Mechanical and durability properties of ultra-high performance concrete incorporated with various nano waste materials under different curing conditions. Journal of Building Engineering, 43: 102569. https://doi.org/10.1016/j.jobe.2021.102569

[5] Dadouch, M., Belal, T., Ghembaza, M.S. (2024). Valorization of glass waste as partial substitution of sand in concrete–Investigation of the physical and mechanical properties for a sustainable construction. Construction and Building Materials, 411: 134436. https://doi.org/10.1016/j.conbuildmat.2023.134436

[6] Ravina, D., Mehta, P.K. (1988). Compressive strength of low cement/high fly ash concrete. Cement and Concrete

Research, 18(4): 571-583. https://doi.org/10.1016/0008-8846(88)90050-6
[7] Wang, D., Jantwal, A., Kaynak, E., Sas, G., Das, O. (2025). Promoting internal curing in concrete by replacing sand with sustainable biochar. Case Studies in Construction Materials, 22: e04542. https://doi.org/10.1016/j.cscm.2025.e04542
[8] Zhang, S., Cao, K., Wang, C., Wang, X., Wang, J., Sun, B. (2020). Effect of silica fume and waste marble powder on the mechanical and durability properties of cellular concrete. Construction and Building Materials, 241: 117980. https://doi.org/10.1016/j.conbuildmat.2019.117980
[9] Awad, A.H., El-gamasy, R., Abd El-Wahab, A.A., Abdellatif, M.H. (2019). Mechanical behavior of PP reinforced with marble dust. Construction and Building Materials, 228: 116766. https://doi.org/10.1016/j.conbuildmat.2019.116766
[10] Özkılıç, Y.O., Zeybek, Ö., Bahrami, A., Celik, A.I., et al. (2023). Optimum usage of waste marble powder to reduce use of cement toward eco-friendly concrete. Journal of Materials Research and Technology, 25: 4799-4819. https://doi.org/10.1016/j.jmrt.2023.06.126
[11] Ravikanth, P., Saravanan, T.J., Kabeer, K.S.A. (2024). Supervised data-driven approach to predict split tensile and flexural strength of concrete with marble waste powder. Cleaner Materials, 11: 100231. https://doi.org/10.1016/j.clema.2024.100231
[12] Wang, Y., Xiao, J., Zhang, J. (2022). Effect of waste marble powder on physical and mechanical properties of concrete. Journal of Renewable Materials, 10(10): 2623-2637. https://doi.org/10.32604/jrm.2022.019381
[13] Ulubeyli, G.C., Bilir, T., Artir, R. (2016). Durability properties of concrete produced by marble waste as aggregate or mineral additives. Procedia Engineering, 161: 543-548. https://doi.org/10.1016/j.proeng.2016.08.689
[14] Bourzik, O., Baba, K., Akkouri, N., Nounah, A. (2023). Effect of waste marble powder on the properties of concrete. Materials Today: Proceedings, 72: 3265-3269. https://doi.org/10.1016/j.matpr.2022.07.184
[15] Norme NF P 18-500. (1995). Béton - Béton de sable. https://www.boutique.afnor.org/fr-fr/norme/nf-p18500/beton-beton-de-sable/fa038712/10614.
[16] Djebien, R., Abbas, Y., Bouabaz, A., Ziada, Y.N. (2022). Shrinkage and absorption of sand concrete containing marble waste powder. Civil and Environmental Engineering Reports, 32(1): 240-254. http://doi.org/10.2478/ceer-2022-0014
[17] Benaissa, I., Nasser, B., Aggoun, S., Malab, S. (2015). Properties of fibred sand concrete sprayed by wet-mix process. Arabian Journal for Science and Engineering, 40(8): 2289-2299. https://doi.org/10.1007/s13369-015-1753-3
[18] Shridevi, P.V., Hameed, M.S., Kumar, R., Dhanalakshmi, A., Ansari, H.M.T. (2023). Strength characteristics of fibre reinforced self compacting concrete using marble sludge powder. Materials Today: Proceedings. https://doi.org/10.1016/j.matpr.2023.12.004
[19] Bayraktar, O.Y., Kaplan, G., Gencel, O., Benli, A., Sutcu, M. (2021). Physico-mechanical, durability and thermal properties of basalt fiber reinforced foamed concrete containing waste marble powder and slag. Construction and Building Materials, https://doi.org/10.1016/j.conbuildmat.2021.123128
[20] Shukla, A., Gupta, N., Kishore, K. (2020). Experimental investigation on the effect of steel fiber embedded in marble dust based concrete. Materials Today: Proceedings, 26: 2938-2945. https://doi.org/10.1016/j.matpr.2020.02.607
[21] Venkataramana, N., Babu, U.R. (2018). Bearing strength of steel fibre reinforced black marble stone waste aggregate concrete. Materials Today: Proceedings, 5(1): 1201-1210. https://doi.org/10.1016/j.matpr.2017.11.202
[22] Karimipour, A., Jahangir, H., Eidgahee, D.R. (2021). A thorough study on the effect of red mud, granite, limestone and marble slurry powder on the strengths of steel fibres-reinforced self-consolidation concrete: Experimental and numerical prediction. Journal of Building Engineering, 44: 103398. https://doi.org/10.1016/j.jobe.2021.103398
[23] Phan, L.T., Carino, N.J. (2002). Effects of test conditions and mixture proportions on behavior of high-strength concrete exposed to high temperatures. ACI Materials Journal, 99(1): 54-66. https://tsapps.nist.gov/publication/get_pdf.cfm?pub_id=860335.
[24] Khodabakhshian, A., De Brito, J., Ghalehnovi, M., Shamsabadi, E.A. (2018). Mechanical, environmental and economic performance of structural concrete containing silica fume and marble industry waste powder. Construction and Building Materials, 169: 237-251. https://doi.org/10.1016/j.conbuildmat.2018.02.192
[25] Vardhan, K., Siddique, R., Goyal, S. (2019). Strength, permeation and micro-structural characteristics of concrete incorporating waste marble. Construction and Building Materials, 203: 45-55. https://doi.org/10.1016/j.conbuildmat.2019.01.079
[26] Gokulnath, V., Ramesh, B., Raghuraman, R. (2020). Study on the effect of M-sand in self-compacting concrete with addition of steel fibers. Materials Today: Proceedings, 22: 843-846. https://doi.org/10.1016/j.matpr.2019.11.029
[27] Cai, B., Chen, H., Xu, Y., Fan, C., Li, H., Liu, D. (2024). Study on fracture characteristics of steel fiber reinforced manufactured sand concrete using DIC technique. Case Studies in Construction Materials, 20: e03200. https://doi.org/10.1016/j.cscm.2024.e03200
[28] Murali, G., Vinodha, E. (2018). Experimental and analytical study of impact failure strength of steel hybrid fibre reinforced concrete subjected to freezing and thawing cycles. Arabian Journal for Science and Engineering, 43(10): 5487-5497. https://doi.org/10.1007/s13369-018-3202-6
[29] Ammari, M.S., Bederina, M., Belhadj, B., Merrah, A. (2020). Effect of steel fibers on the durability properties of sand concrete with barley straws. Construction and Building Materials, 264: 120689. https://doi.org/10.1016/j.conbuildmat.2020.120689
[30] Jiao, Y., Yang, H., Wang, J., Fang, M., Shi, H. (2024). Effects of fiber properties on flexural and fracture characteristics of manufactured sand concrete based on acoustic emission. Journal of Building Engineering, 84: 108308. https://doi.org/10.1016/j.jobe.2023.108308
[31] Durgun, M.Y., Sevinc, A.H. (2025). Comparative study of concrete properties using basalt, barite, pumice, and marble aggregates subjected to extreme temperatures.

Journal of Building Engineering, 113: 114036. https://doi.org/10.1016/j.jobe.2025.114036
[32] Ahmad, J., Zhou, Z., Alattyih, W., Naqash, M.T. (2025). Performance of steel-fibre-reinforced self-compacting concrete subjected to high temperature. Magazine of Concrete Research, 77(3-4): 228-240. https://doi.org/10.1680/jmacr.24.00172
[33] Billhout, H. (1994). Béton de sable: Caractéristiquesetpratiquesd'utilisation. Projet National de Recherche de Développement SABLOCRETE, Université de Paris, Presse de l'Ecole des Ponts et Chaussées, 121p.
[34] NF, P. (1981). P 18-404: Bétons–Essais d'étude de convenance et de contrôle–Confection et conservation des éprouvettes. AFNOR, Paris, décembre.
[35] Eurocode 2: Design of concrete structures. https://eurocodes.jrc.ec.europa.eu/EN-Eurocodes/eurocode-2-design-concrete-structures.
[36] Eurocode 1: Actions on structures. https://eurocodes.jrc.ec.europa.eu/EN-Eurocodes/eurocode-1-actions-structures.
[37] BS EN 12504-4:2021. Testing concrete in structures determination of ultrasonic pulse velocity. https://www.en-standard.eu/bs-en-12504-4-2021-testing-concrete-in-structures-determination-of-ultrasonic-pulse-velocity/.
[38] NF EN 12390-3. Essais pour béton durci - Partie 3: Résistance à la compression des éprouvettes. https://www.boutique.afnor.org/fr-fr/norme/nf-en-123903/essais-pour-beton-durci-partie-3-resistance-a-la-compression-des-eprouvette/fa190566/83462.
[39] NF EN 12390-5. Essais pour béton durci - Partie 5: Résistance à la flexion sur éprouvettes. https://www.boutique.afnor.org/fr-fr/norme/nf-en-123905/essais-pour-beton-durci-partie-5-resistance-a-la-flexion-sur-eprouvettes/fa155371/39062.
[40] Wang, J., Niu, D. (2016). Influence of freeze–thaw cycles and sulfate corrosion resistance on shotcrete with and without steel fiber. Construction and Building Materials, 122: 628-636. https://doi.org/10.1016/j.conbuildmat.2016.06.100
[41] Kabbo, M.K.I., Sobuz, M.H.R., Aditto, F.S., Khan, M.H., et al. (2025). Experimental assessment and machine learning quantification of structural eco-cellular lightweight concrete incorporating waste marble powder and silica fume. Journal of Building Engineering, 105: 112557. https://doi.org/10.1016/j.jobe.2025.112557
[42] Ahmad, J., Zhou, Z. (2024). Waste marble based self compacting concrete reinforced with steel fiber exposed to aggressive environment. Journal of Building Engineering, 81: 108142. https://doi.org/10.1016/j.jobe.2023.108142
[43] Pliya, P., Beaucour, A.L., Noumowé, A. (2011). Contribution of cocktail of polypropylene and steel fibres in improving the behaviour of high strength concrete subjected to high temperature. Construction and Building Materials, 25(4): 1926-1934. https://doi.org/10.1016/j.conbuildmat.2010.11.064
[44] Poon, C.S., Azhar, S., Anson, M., Wong, Y.L. (2001). Strength and durability recovery of fire-damaged concrete after post-fire-curing. Cement and Concrete Research, 31(9): 1307-1318. https://doi.org/10.1016/S0008-8846(01)00582-8
[45] Belaribi, H. (2019). L'influence des types de fibres sur le comportement du béton à haute temperature. Doctoral dissertation. Université Mohamed Khider-Biskra. http://thesis.univ-biskra.dz/id/eprint/4354.

APPENDIX

Table A1. Statistical variability of compressive strength at 20 ℃

	Without Steel Fibre Reinforcement		
Curing Age, Days	**Compressive Strength, N/mm²**	**Average, N/mm²**	**Standard Deviation, N/mm²**
	35.63		
7	39.27	38.51	2.59
	40.63		
	41.26		
14	41.59	41.65	0.43
	42.11		
	41.17		
28	47.15	42.24	4.47
	38.4		

Table A2. Statistical variability of compressive strength at 20 ℃ (0.25% steel fibre reinforcement)

	With 0.25% Steel Fibre Reinforcement		
Curing Age, Days	**Compressive Strength, N/mm²**	**Average, N/mm²**	**Standard Deviation, N/mm²**
	35.63		
7	39.27	28.09	2.51
	40.63		
	35.64		
14	38.99	37.32	2.37
	-		
28	39.18	-	-

Table A3. Statistical variability of compressive strength at 20 ℃ (0.50% steel fibre reinforcement)

With 0.50% Steel Fibre Reinforcement			
Curing Age, Days	**Compressive Strength, N/mm²**	**Average, N/mm²**	**Standard Deviation, N/mm²**
	28.91		
7	30.36	29.35	0.88
	28.79		
	45.63		
14	28.96	34.80	9.39
	29.81		
	40.34		
28	48.18	44.84	4.05
	45.99		

Table A4. Statistical variability of compressive strength at 20 ℃ (0.75% steel fibre reinforcement)

With 0.75% Steel Fibre Reinforcement			
Curing Age, Days	**Compressive Strength, N/mm²**	**Average, N/mm²**	**Standard Deviation, N/mm²**
	36.41		
7	40.15	39.62	2.98
	42.30		
	39.86		
14	43.71	40.36	3.13
	37.51		
	44.62		
28	43.48	45.06	1.83
	47.07		

Table A5. Statistical variability of tensile strength at 20 ℃

Without Steel Fibre Reinforcement			
Curing Age, Days	**Tensile Strength, N/mm²**	**Average, N/mm²**	**Standard Deviation, N/mm²**
	7.67		
7	7.39	7.576	0.16
	7.67		
	7.65		
14	7.60	7.722	0.17
	7.91		
	8.68		
28	8.06	8.425	0.33
	38.4		

Table A6. Statistical variability of tensile strength at 20 ℃ (0.25% steel fibre reinforcement)

With 0.25% Steel Fibre Reinforcement			
Curing Age, Days	**Tensile Strength, N/mm²**	**Average, N/mm²**	**Standard Deviation, N/mm²**
	8.565		
7	8.115	8.545	0.42
	8.956		
	8.555		
14	8.57	8.56	0.01
	-		
	9.261		
28	8.649	9.36	0.77
	10.18		

Table A7. Statistical variability of tensile strength at 20 ℃ (0.50% steel fibre reinforcement)

With 0.50% Steel Fibre Reinforcement			
Curing Age, Days	**Tensile Strength, N/mm²**	**Average, N/mm²**	**Standard Deviation, N/mm²**
	7.78		
7	8.81	8.090	0.63
	7.68		
	8.2		
14	-	8.200	
	-		
	8.999		
28	8.81	8.555	0.61
	7.857		

Table A8. Statistical variability of tensile strength at 20 ℃ (0.75% steel fibre reinforcement)

	With 0.75% Steel Fibre Reinforcement		
Curing Age, Days	**Tensile Strength, N/mm²**	**Average, N/mm²**	**Standard Deviation, N/mm²**
7	- 7.882 -	7.88	
14	8.45 - -	8.45	
28	8.649 8.68 -	8.66	0.02

Table A9. Statistical variability of compressive strength at 600 ℃

	28 Day Compressive Strength at 600 ℃: Plain vs Steel-Fibre-Reinforced		
Fibre Content, %	**Compressive Strength, N/mm²**	**Average, N/mm²**	**Standard Deviation, N/mm²**
0.00	26.16 8.78 25.52	26.96	1.99
0.25	25.10 24.28 24.61	24.67	0.41
0.50	23.31 27.15 29.23	26.57	3.01
0.75	19.87 24.25 21.90	22.01	2.19

Table A10. Statistical variability of mass loss

Fibre Content, %	**20 ℃**	**600 ℃**	**Mean at 20 ℃**	**Mean at 600 ℃**	**Mass Loss, %**
0.00	4020.00 3961.00 4061.00	2019 2007 2047	4014	2177	8.93
0.25	2227.8 2195.4 2188.8	2041 2001 2010	2204	2017	8.48
0.50	2217.6 2189.0 2187.7	2019 2007 2047	2198	2024	7.91
0.75	2190.8 2170.7 2151.9	2055 1997 2016	2171	2023	6.83

Table A11. Statistical variability of tensile strength at 600 ℃

	28 Day Tensile Strength at 600 ℃: Plain vs Steel-Fibre-Reinforced		
Fibre Content, %	**Tensile Strength, N/mm²**	**Average, N/mm²**	**Standard Deviation, N/mm²**
0.00	1.95 -	1.95	
0.25	4.5 3 3	3.50	0.87
0.50	2.7 2.4	2.63	0.21
0.75	2.8 3	2.77	0.68

Table A12. Statistical variability of ultrasonic velocity

Fibre Content, %	20 ℃	600 ℃	Mean at 20 ℃	Mean at 600 ℃
0.00	4494	2180	4494	2177
	4494	2174		
0.25	4545	1934	4535	1923
	4525	1912		
0.50	4525	2066	4505	2092
	4484	2119		
0.75	4149	2119	4230	2017
	4310	1916		